Cardiac Expression of Human Type 2 Iodothyronine Deiodinase Increases Glucose Metabolism and Protects Against Doxorubicin-induced Cardiac Dysfunction in Male Mice

Eun-Gyoung Hong, Brian W. Kim, Dae Young Jung, Jong Hun Kim, Tim Yu, Wagner Seixas Da Silva, Randall H. Friedline, Suzy D. Bianco, Stephen P. Seslar, Hiroko Wakimoto, Charles I. Berul, Kerry S. Russell, Ki Won Lee, P. Reed Larsen, Antonio C. Bianco, and Jason K. Kim

Section of Endocrinology, Metabolism (K.-G.H., T.Y., J.K.K.), and Cardiovascular Medicine (K.S.R.), Department of Internal Medicine, Yale University School of Medicine, New Haven, Connecticut 06520; Department of Endocrinology and Metabolism (E.-G.H.), Dongtan Sacred Heart Hospital, Hallym University College of Medicine, Gyeonggi-do, South Korea; Thyroid Section (B.W.K., W.S.D.S., P.R.L., A.C.B.), Brigham and Women's Hospital, and Department of Genetics (H.W.), Harvard Medical School, Boston, Massachusetts 02115; Division of Endocrinology, Diabetes, and Metabolism (B.W.K., S.D.B., A.C.B.), University of Miami, Miller School of Medicine, Miami, Florida 33101; Program in Molecular Medicine (D.Y.J., J.H.K., R.H.F., J.K.K.) and Division of Endocrinology, Metabolism, and Diabetes (J.K.K.), Department of Medicine, University of Massachusetts Medical School, Worcester, Massachusetts 01605; Department of Cardiology (S.P.S.), Seattle Children's Hospital, University of Washington School of Medicine, Seattle, Washington 98105; Department of Cardiology (C.I.B.), Children's National Medical Center, Washington, DC 20010; and World Class University Biomodulation Major (J.H.K., K.W.L.), Department of Agricultural Biotechnology and Center for Food and Bioconvergence, Seoul National University, Seoul, Republic of Korea

Altered glucose metabolism in the heart is an important characteristic of cardiovascular and metabolic disease. Because thyroid hormones have major effects on peripheral metabolism, we examined the metabolic effects of heart-selective increase in T3 using transgenic mice expressing human type 2 iodothyronine deiodinase (D2) under the control of the α-myosin heavy chain promoter (MHC-D2). Hyperinsulinemic-euglycemic clamps showed normal whole-body glucose disposal but increased hepatic insulin action in MHC-D2 mice as compared to wild-type (WT) littermates. Insulin-stimulated glucose uptake in heart was not altered, but basal myocardial glucose metabolism was increased by more than two-fold in MHC-D2 mice. Myocardial lipid levels were also elevated in MHC-D2 mice, suggesting an overall up-regulation of cardiac metabolism in these mice. The effects of doxorubicin (DOX) treatment on cardiac function and structure were examined using M-mode echocardiography. DOX treatment caused a significant reduction in ventricular fractional shortening and resulted in more than 50% death in WT mice. In contrast, MHC-D2 mice showed increased survival rate after DOX treatment, and this was associated with a six-fold increase in myocardial glucose metabolism and improved cardiac function. Myocardial activity and expression of AMPK, GLUT1, and Akt were also elevated in MHC-D2 and WT mice following DOX treatment. Thus, our findings indicate an important role of thyroid hormone in cardiac metabolism and further suggest a protective role of glucose utilization in DOX-mediated cardiac dysfunction. **(*Endocrinology* 154: 3937–3946, 2013)**

ISSN Print 0013-7227 ISSN Online 1945-7170
Printed in U.S.A.

Received December 21, 2012. Accepted July 9, 2013.
First Published Online July 16, 2013

Abbreviations: AMPK, 5′AMP-activated protein kinase; BNP, B-type natriuretic peptide; D2, iodothyronine deiodinase; DOX, doxorubicin; ECG, electrocardiogram; FS, fractional shortening; GLUT, glucose transporter; HGP, hepatic glucose production; MHC, α-myosin heavy chain; MHC-D2, α-myosin heavy chain promoter ; WT, wild type.

Alterations in myocardial glucose metabolism and insulin action are major characteristics of cardiovascular and metabolic disease (1, 2). Although mitochondrial lipid oxidation is the principal energy source for the normal heart, maintenance of glucose metabolism is important for normal cardiac function (3). It is well known that a failing heart undergoes a change in substrate utilization with greater dependence on glucose as energy source (4). Because type 2 diabetes is characterized by impaired glucose metabolism, diabetic heart is likely to be more sensitive to cellular damage under stress conditions.

The effect of thyroid hormone on basal metabolism and energy expenditure is well known (5, 6). Altered levels of thyroid hormones have been associated with insulin resistance, blunted insulin secretion, and obesity (7–9). Type 2 iodothyronine deiodinase (D2) is an important modulator of local thyroid hormone signaling by catalyzing the intracellular conversion of T4 to the active T3 form. A common Thr92Ala polymorphism in the gene encoding D2 (*Dio2*) has been associated with reduced glucose turnover in nondiabetic subjects (10). Mice with targeted deletion of *Dio2* gene has been shown to be less adaptive to cold stress due to impaired thermogenesis in brown adipose tissue (11). These mice were also shown to develop insulin resistance and become more obese in response to high-fat feeding (12). These studies clearly demonstrate an important role of thyroid hormone signaling in systemic metabolism and energy expenditure.

The cardiovascular phenotypes of excess thyroid hormone include increases in heart rate, cardiac output, coronary blood flow, and oxygen consumption in heart (13). Recently, mice with heart-specific expression of human D2 under the control of the α-myosin heavy chain (MHC) promoter (MHC-D2) were generated and shown to have tachycardia with altered levels of high-energy phosphate compounds during isolated perfusion (14, 15). Furthermore, doxorubicin (DOX) is an anthracycline chemotherapeutic agent that is effectively used in treating multiple types of cancer, but its use has been limited by undesirable cardiotoxic effects (16, 17). For this reason, a cohort of studies have attempted to understand the cardiotoxic mechanism of DOX and to attenuate such effects using animal models (18, 19). Soni and colleagues found that DOX-mediated cardiotoxicity involved increased levels of caspase-3 and reduced total antioxidant status in mice (20). Another study reported that aryl hydrocarbon receptor and formation of free radicals mediate DOX-induced cardiotoxicity in mice (18). In the current study, we examined the metabolic effects of excess thyroid hormones in heart and further determined the effects of DOX treatment in MHC-D2 mice.

Materials and Methods

Body composition and energy balance measurement

Male mice with heart-specific expression of human D2 (MHC-D2) and wild-type littermates (WT) were obtained from Dr Antonio Bianco and housed at the animal facility with controlled temperature (23°C) and lighting (12-h light, 0700–1900 h; 12-h dark, 1900–0700 h). Body composition was noninvasively measured using ^{1}H-MRS (Echo Medical Systems, Houston, Texas). The animal studies were approved by the Institutional Animal Care and Use Committee of the Yale University School of Medicine and University of Massachusetts Medical School.

Hyperinsulinemic-euglycemic clamp to assess insulin sensitivity in conscious mice

At 4 to 5 days before clamp experiments, a survival surgery was performed to establish indwelling catheter in jugular vein. On the day of experiment, male MHC-D2 mice and WT littermates (n = 4 for each group) were fasted overnight (~15 h), and a 2-hour hyperinsulinemic-euglycemic clamp was conducted in conscious mice with a primed and continuous infusion of human insulin (150 mU/kg body weight priming followed by 2.5 mU/kg/min; Novolin; Novo Nordisk, Bagsværd, Denmark) (21). To maintain euglycemia, 20% glucose was infused at variable rates during clamps. Whole-body glucose turnover was assessed with a continuous infusion of [3-^{3}H]glucose (PerkinElmer, Waltham, Massachusetts), and 2-deoxy-D-[1-^{14}C]glucose was administered as a bolus (10 μCi) at 75 minutes after the start of clamps to measure insulin-stimulated glucose uptake in individual organs. At the end of the clamps, mice were anesthetized, and tissues were taken for biochemical analysis (21).

Basal glucose and lipid metabolism in mice

Male MHC-D2 mice and WT littermates were used to measure in vivo basal glucose metabolism (n = 7 for each group). Basal glucose uptake in individual organs was measured using a bolus injection of 2-deoxy-D-[1-^{14}C]glucose (30 μCi) in awake mice and taking tissue samples 30 minutes later for analysis (22).

In another cohort of male MHC-D2 mice and WT littermates (n = 4 for each group), [^{3}H]palmitate was bolus injected (30 μCi) in awake mice, and blood samples were taken at 0.5, 1, 2, 3, 4, and 5 minutes after injection for determination of plasma concentration of [^{3}H]palmitate as a measure of systemic lipid clearance.

Biochemical analysis

Glucose concentrations during clamps were analyzed using 5 μL plasma by a glucose oxidase method on Analox GM9 Analyzer (Analox Instruments Ltd, Hammersmith, London, United Kingdom). Plasma concentrations of [3-^{3}H]glucose, 2-[^{14}C]DG, and $^{3}H_2O$ were determined following deproteinization of plasma samples as previously described (21). For the determination of tissue 2-[^{14}C]DG-6-phosphate content, tissue samples were homogenized, and the supernatants were subjected to an ion-exchange column to separate 2-[^{14}C]DG-6-P from 2-[^{14}C]DG. Insulin-stimulated glucose uptake in individual tissues was assessed by determining the tissue content of 2-[^{14}C]DG-6-P and plasma 2-[^{14}C]DG profile. Tissue triglycer-

ide concentrations were determined by digesting heart samples obtained from MHC-D2 and WT mice in chloroform-methanol and using a triglyceride assay kit (Sigma, St Louis, Missouri).

Western blot analysis

Total protein expression and phosphorylation of glucose transporter 1 (GLUT1), GLUT4, Akt/PKB, and 5′AMP-activated protein kinase (AMPK) were determined using Western blots in heart samples obtained from MHC-D2 and WT mice at baseline and after DOX treatment. Fifty milligrams of heart tissues were lysed in 500 μL of ice-cold lysis buffer, T-PER tissue protein extraction reagent (Thermo Rockford, Illinois) containing phosphatase inhibitor cocktail (Sigma-Aldrich, St Louis, Missouri), protease inhibitor cocktail (Roche, Indianapolis, Indiana), and phenylmethanesulfonyl fluoride (Sigma-Aldrich). Tissue lysates were blended with homogenizer Ultra-Turrax T25 (Janke and Kunkel, IKA Labortechnik, Stauten, Germany), incubated on ice for 2 hours, and centrifuged at 12 000 rpm, 4°C for 15 minutes. The supernatants were harvested, and protein concentrations were determined using the BCA reagent (Pierce, Rockford, Illinois). Fifty milligrams of protein of each sample was mixed with 6× sample loading buffer, heated for 5 minutes at 95°C, and loaded in 10% or 12% gel for SDS-PAGE. After SDS-PAGE, proteins were transferred to polyvinylidene difluoride membranes (Bio-Rad, Berkeley, California). Membranes were blocked with 5% skim milk in Tris-buffered saline with Tween 20 for 1 hour at room temperature and incubated with GLUT1 (Millipore, Billerica, Massachusetts), GLUT4 (Cell Signaling, Danvers, Massachusetts), Thr^{172}-phospho-AMPK (Cell Signaling), AMPK (Cell Signaling), Ser^{473}-phospho-Akt (Cell Signaling), or Akt (Cell Signaling) antibodies in Tris-buffered saline with Tween 20 containing 5% skim milk or BSA for overnight at 4°C. Detection of immunoreactive bands was achieved using enhanced chemiluminescent substrate (Thermo) and the images of the bands were taken by Biospectrum (UVP, Upland, California). Quantification analysis of the bands was performed using ImageJ (National Institutes of Health, Bethesda, Maryland).

DOX treatment and echocardiography to assess cardiac structure and function in mice

Mice received an ip injection of DOX (15 mg/kg body weight). M-mode echocardiography was performed using the Philips Sonos 5500 System (Philips, Aliso Viejo, California) with a 15-MHz probe in mice lightly anesthetized with inhaled isoflurane. The images were collected in the short and long axes, and the data represent the averaged values of three to five cardiac cycles as previously described (23).

Calculation

Rates of basal hepatic glucose production (HGP) and insulin-stimulated whole-body glucose turnover were determined as previously described (21). Insulin-stimulated rate of HGP during clamp was determined by subtracting the glucose infusion rate from whole-body glucose uptake. Insulin-stimulated glucose uptake in individual tissues was assessed by determining the tissue (eg, skeletal muscle, heart) content of 2-[^{14}C]DG-6-phosphate and plasma 2-[^{14}C]DG profile.

Statistics

Data are expressed as means ± SE. The significance of the difference in mean values between MHC-D2 mice versus WT mice was evaluated using the Student's *t* test. The statistical significance was at the $P < .05$ level.

Results

Metabolic characterization of mice with heart-selective expression of human D2

MHC-D2 mice showed normal body weight, and ^{1}H-MRS analysis found comparable whole-body fat mass and lean mass between MHC-D2 and WT mice (Figure 1, A–C). Basal plasma insulin levels were measured after an overnight fast (~17 h) and found to be similar between MHC-D2 and WT mice (Figure 1D). Basal plasma glucose levels were also normal in MHC-D2 mice (7.3 ± 1.2 mM).

A 2-hour hyperinsulinemic-euglycemic clamp was performed in conscious mice by raising plasma insulin levels two- to three-fold above basal in both groups of mice, and euglycemia (~7 mM) was maintained using a variable infusion of 20% glucose during the clamp (Figure 1D). Steady-state glucose infusion rate to maintain euglycemia during clamps was not significantly different between MHC-D2 and WT mice (Figure 1E). Insulin-stimulated whole-body glucose turnover was measured using a continuous infusion of [3-^{3}H]glucose and found to be unaltered in MHC-D2 mice, indicating that heart-selective expression of human D2 does not affect systemic insulin sensitivity (Figure 1F). Basal rate of HGP was not significantly altered in MHC-D2 mice (Figure 1G). In contrast, HGP was more significantly suppressed by insulin during clamp in MHC-D2 mice, resulting in a lower rate of clamp HGP (Figure 1H). As a result, hepatic insulin action was increased by two-fold in MHC-D2 mice as compared to WT mice (Figure 1I).

Cardiac energy metabolism in MHC-D2 mice

Using a bolus injection of 2-[^{14}C]DG during clamps, we measured insulin-stimulated glucose uptake in individual organs. Insulin-stimulated glucose uptake in heart was not altered in MHC-D2 mice (Figure 2A). Basal myocardial glucose uptake was measured using 2-[^{14}C]DG injection at basal state, and heart-selective expression of human D2 caused a two- to three-fold increase in basal glucose uptake in heart (Figure 2B). Increased myocardial glucose metabolism was not due to altered expression of proteins involved in glucose trafficking because myocardial GLUT1 levels were not different in MHC-D2 mice (Figure 2D).

Lipid metabolism was examined in MHC-D2 and WT mice. Myocardial triglyceride levels were significantly in-

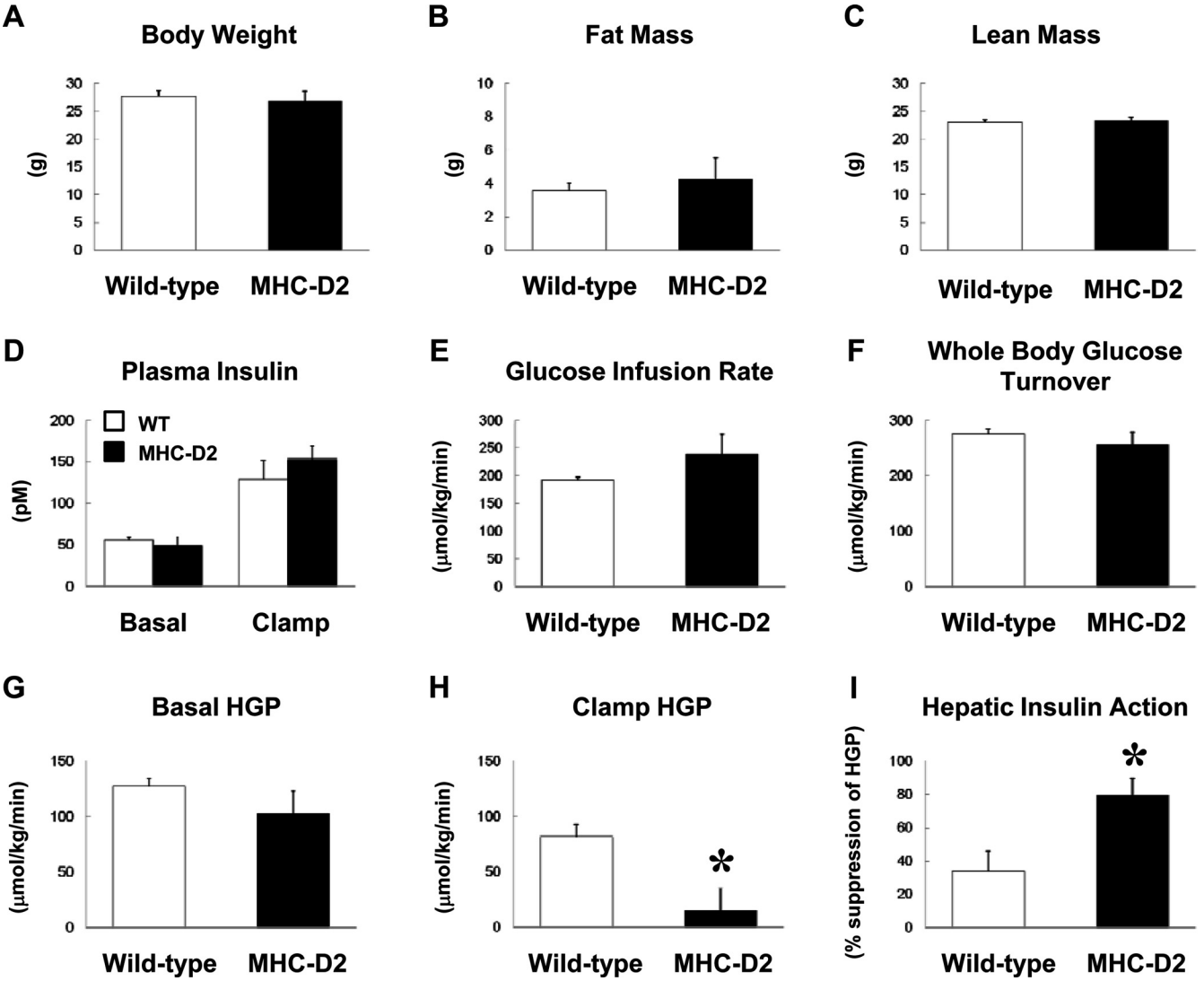

Figure 1. Metabolic effects of heart-selective increase in T3. Body composition analysis and a 2-hour hyperinsulinemic-euglycemic clamp was performed in male transgenic mice with heart-selective expression of human D2 (MHC-D2) mice and WT littermates (n = 4 per group). (A) Body weight. (B, C) Whole-body fat mass and lean mass, measured using ^{1}H-MRS, in mice. (D) Plasma insulin levels in overnight-fasted state (basal) and during euglycemic clamp. (E) Steady-state glucose infusion rates required to maintain euglycemia during clamps. (F) Insulin-stimulated whole-body glucose turnover. (G) Basal rate of HGP in mice. (H) HGP during hyperinsulinemic-euglycemic clamp. (I) Hepatic insulin action expressed as insulin-mediated percentage suppression of basal HGP. Data are presented as means ± SE. *, $P < .05$ vs WT mice.

creased in MHC-D2 mice compared with WT mice (Figure 2C). We performed a bolus injection of [^{3}H]palmitate and found that systemic clearance of [^{3}H]palmitate was increased in MHC-D2 mice as compared to WT mice, suggesting enhanced lipid metabolism in MHC-D2 mice (Figure 2E). As a measure of de novo lipogenesis, [^{3}H]glucose conversion into myocardial triglyceride also tended to increase in MHC-D2 mice (Figure 2F).

To examine the cardiac-specific nature of these metabolic effects in MHC-D2 mice, we measured basal glucose uptake in white adipose tissue (epididymal), which was not altered in MHC-D2 mice (Figure 2G). In addition, intrahepatic triglyceride levels were comparable between MHC-D2 mice and WT littermates (Figure 2H).

Effects of DOX treatment on cardiac structure and function in MHC-D2 mice

Because basal myocardial metabolism was up-regulated in MHC-D2 mice, we examined the effects of DOX treatment on cardiac structure and function in MHC-D2 mice. DOX was injected ip into MHC-D2 and WT mice at day 0, and WT mice began to die starting at 6 days after DOX treatment (Figure 3A). At 8 days after DOX treatment, more than 50% of WT mice had died. In contrast, all of the MHC-D2 mice survived at 8 days after DOX treatment, and there was a gradual decline in survival rate of MHC-D2 mice after 9 days of DOX treatment (Figure 3A).

At 12 days after DOX treatment, we measured basal myocardial glucose metabolism in the remaining WT and

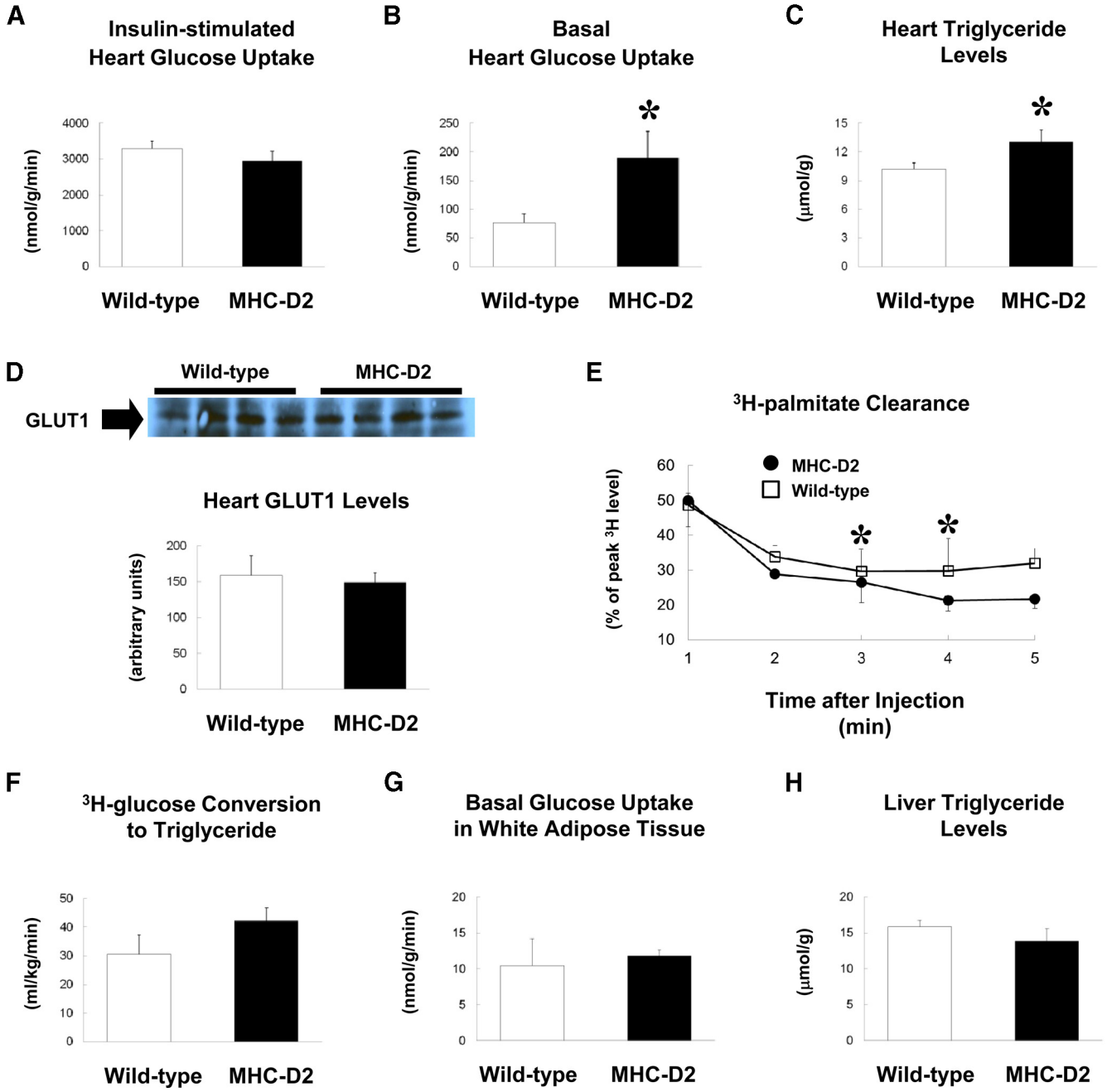

Figure 2. Myocardial glucose and lipid metabolism in MHC-D2 mice. Basal and insulin-stimulated glucose uptake in heart was measured following iv injection of 2-[^{14}C]DG in MHC-D2 mice and WT littermates. (A) Insulin-stimulated glucose uptake in heart (n = 4 for each group). (B) Basal glucose uptake in heart (n = 7 for each group). (C) Myocardial triglyceride levels (n = 4–6). (D) GLUT1 expression in heart samples was measured using Western blot. (E) Systemic clearance of [^{3}H]-palmitate following a bolus injection (n = 4 for each group). (F) ^{3}H-glucose conversion into myocardial triglyceride (n = 4–6). (G) Basal glucose uptake in white adipose tissue (epididymal) (n = 3 for each group). (H) Intrahepatic triglyceride levels (n = 4–6). Data are presented as means ± SE. *, $P < .05$ vs WT mice.

MHC-D2 mice. Our data indicate that basal glucose uptake in heart was elevated by more than six-fold in MHC-D2 mice compared to WT littermates (2085 ± 273 nmol/g/min in MHC-D2 mice vs 487 ± 50 nmol/g/min in WT mice after DOX treatment; Figure 3B). Although basal myocardial glucose uptake was elevated in both groups of mice following DOX treatment, more dramatic effects in MHC-D2 mice may be due to enhanced myocardial glucose metabolism associated with increased D2 activity and cardiac work in these mice.

Cardiac structure and function were assessed using M-mode echocardiography before DOX treatment (baseline) and 8 days after DOX treatment in surviving WT and MHC-D2 mice. At baseline (before DOX treatment), MHC-D2 mice showed normal cardiac structure and function with various parameters that are comparable to

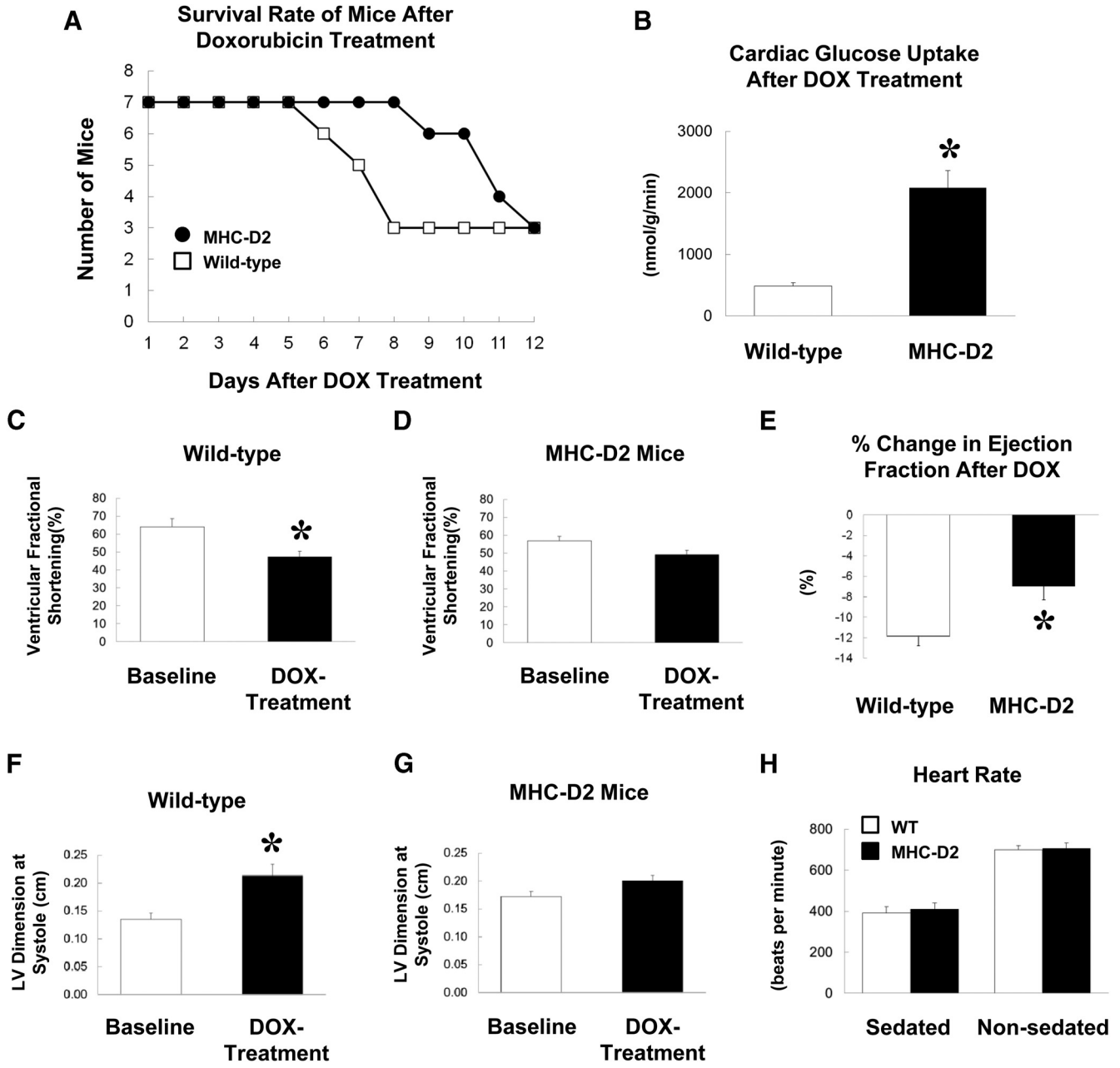

Figure 3. Effects of DOX treatment in MHC-D2 mice. Metabolic and cardiac studies were performed in MHC-D2 mice and WT littermates following ip injection of DOX (n = 7 for each group). (A) Survival rate of mice after DOX treatment. (B) Basal glucose uptake in heart 12 days after DOX treatment (n = 3 for each group). *, $P < .05$ vs WT mice. (C) Ventricular FS at baseline (before DOX treatment; n = 7) and 8 days after DOX treatment (n = 3) in WT mice. *, $P < .05$ vs baseline data. (D) Ventricular FS at baseline (before DOX treatment; n = 7) and 8 days after DOX treatment (n = 3) in MHC-D2 mice. (E) Percentage change in EF after DOX treatment in WT and MHC-D2 mice. *, $P < .05$ vs WT mice. (F) Left ventricular (LV) dimension at systole at baseline (before DOX treatment; n = 7) and 8 days after DOX treatment (n = 3) in WT mice. *, $P < .05$ vs baseline data. (G) Left ventricular dimension at systole at baseline (before DOX treatment; n = 7) and 8 days after DOX treatment (n = 3) in MHC-D2 mice. (H) Heart rates were measured noninvasively using ambulatory ECG telemetry in nonsedated, freely moving mice (n = 5 for WT and MHC-D2 mice) and using ECG electrodes in sedated mice (n = 7 for each group). Data are presented as means ± SE.

those of WT mice. After DOX treatment, ventricular fractional shortening (FS) was reduced by 27% in WT mice (64 ± 4% at baseline vs 47 ± 3% after DOX treatment, $P = .04$; Figure 3C). In contrast, there was no significant effect of DOX treatment on ventricular fractional shortening in MHC-D2 mice (57 ± 3% at baseline vs 49 ± 3% after DOX treatment, $P > .05$; Figure 3D). Ejection fraction was reduced following DOX treatment in both groups of mice, but the percentage change in ejection fraction was significantly lower in MHC-D2 mice compared to WT mice (Figure 3E). Left ventricular dimension at systole was increased by 54% in WT mice after DOX treatment (0.14 ± 0.01 cm at baseline vs 0.21 ± 0.02 after DOX treatment, $P = .01$; Figure 3F). In contrast, there was

no significant change in left ventricular dimension after DOX treatment in MHC-D2 mice (0.17 ± 0.01 cm at baseline vs 0.20 ± 0.01 cm after DOX treatment, $P > .05$; Figure 3G). Although some of the effects of DOX treatment on cardiac structure/function are modest in these surviving mice, it is likely that there were more pronounced effects of DOX treatment in those mice that did not survive at the time of measurement.

In a group of age- and weight-matched WT and MHC-D2 mice (31.7 ± 1.1 g and 32.3 ± 1.2 g body weight, respectively), basal heart rates were measured in noninvasive (nonsedated) and sedated states. Briefly, basal heart rates were measured noninvasively using ambulatory electrocardiographic (ECG) telemetry in unrestrained, freely moving mice days after recovery from surgery for transmitter implant (24). Additional heart rates were measured using ECG electrodes in anesthetized mice (25). Our data indicate that basal heart rates at either state were not different between WT and MHC-D2 mice (Figure 3H).

Molecular mechanism of increased glucose metabolism following DOX treatment

To determine the mechanism of DOX-mediated increase in myocardial glucose metabolism, we measured expression of metabolic signaling proteins using Western blot analysis in heart samples obtained from WT and MHC-D2 mice at baseline and after DOX treatment. AMPK, a serine-threonine kinase, is an important regulator of cardiac energy metabolism (26). Thr^{172}-phosphorylation of AMPK in heart was increased by more than six-fold in MHC-D2 mice following DOX treatment as compared to untreated MHC-D2 mice (Figure 4A). Although P-AMPK also increased by ~70% in WT heart following DOX treatment, this difference did not reach a statistical significance ($P = .10$). Total GLUT1 protein levels were also increased by nearly two-fold in MHC-D2 mice following DOX treatment (Figure 4B). In contrast, total GLUT4 and GLUT1 protein levels in WT heart were not affected by DOX treatment. Furthermore, total Akt protein levels and Ser^{473}-phosphorylation of AKT were significantly elevated in WT heart following DOX treatment (Figure 4, C and D). As a result, the ratio of P-Akt to Akt tended to increase by ~30% in WT heart after DOX treatment (Figure 4E). Thus, DOX treatment induced a dramatic activation of key signaling proteins involved in glucose metabolism in heart.

Discussion

The present study shows that heart-selective expression of human D2 and a local increase in T_3 have a major effect on myocardial metabolism. Basal glucose uptake in heart was selectively up-regulated without changes in cardiac insulin action in MHC-D2 mice. DOX treatment caused a significant decrease in ventricular FS and cardiac dysfunction in WT mice. In contrast, MHC-D2 mice showed increased rate of survival following DOX treatment, and this was associated with improved cardiac function/structure and increases in metabolic signaling pathways and glucose metabolism in heart.

It is well known that thyroid hormones regulate metabolism, and hyperthyroidism is associated with insulin resistance and type 2 diabetes (7, 8). Laville and colleagues found that experimental hyperthyroidism increased basal rates of endogenous glucose production and glucose utilization but reduced insulin-mediated suppression of endogenous glucose production in healthy humans (27). Brunetto et al also found that T3 increases skeletal muscle glucose utilization by enhancing GLUT4 intrinsic activity in rats (28). Castillo et al recently found that mice lacking D2 develop obesity, insulin resistance, and hepatic steatosis (29). In the current study, MHC-D2 mice did not show alterations in glucose homeostasis as reflected by normal glucose and insulin levels and whole-body glucose turnover during hyperinsulinemic-euglycemic clamps. This is likely due to the fact that human D2 is selectively expressed in the heart and thus raises only local levels of T3 in MHC-D2 mice. This is important because any changes in glucose homeostasis secondarily affect circulating insulin, which has known inotropic effects in heart (30). Interestingly, HGP during hyperinsulinemic-euglycemic clamp was significantly lower in MHC-D2 mice compared to WT littermates. This increase in hepatic insulin sensitivity was not expected because human D2 expression and T_3 increase were selective to heart in MHC-D2 mice. One potential mechanism may involve myocardial expression and secretion of B-type natriuretic peptide (BNP), which was recently shown to regulate brown fat thermogenesis and metabolism (31). This study found that BNP increased brown fat metabolism by up-regulating uncoupling protein 1 and PGC-1α expression in adipose tissue (31). These effects would increase mitochondrial content and mitochondrial function in cells. Furthermore, BNP is a well-known hormone secreted by cardiomyocytes in response to stress and is commonly used as a clinical marker of failing heart (32). Our findings suggest that altered myocardial energetics may be a possible trigger for BNP release, which may secondarily affect hepatic insulin sensitivity in MHC-D2 mice. Alternatively, BNP release may be triggered by changes in myocardial energy demand due to higher D2 activity and cardiac work in MHC-D2 mice. Additional studies are needed to determine the potential

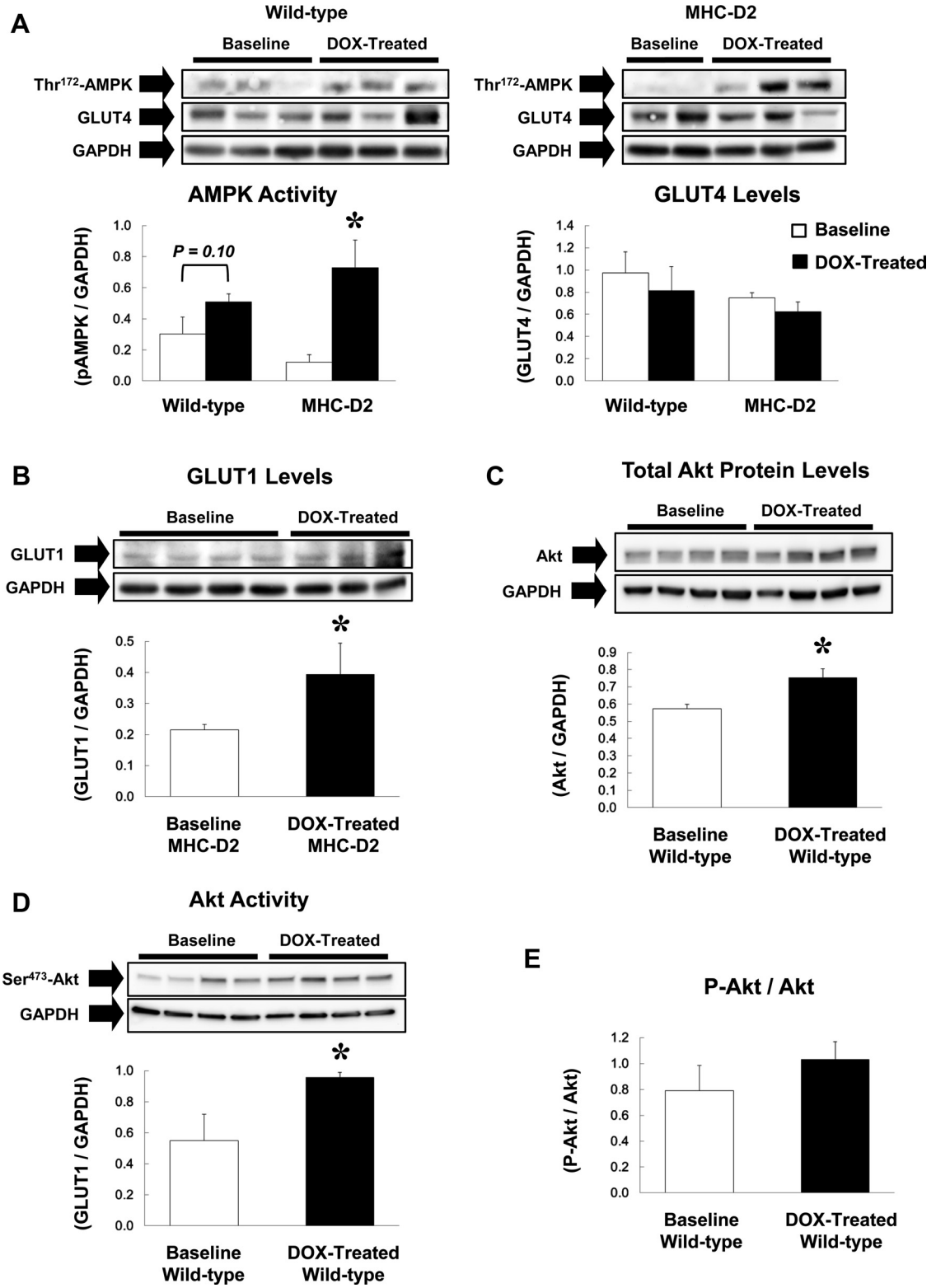

Figure 4. Metabolic signaling pathways following DOX treatment in MHC-D2 and WT mice. Metabolic signaling pathways were examined using Western blot analysis in heart samples obtained at baseline and following DOX treatment in MHC-D2 and WT mice (n = 3–4 for each group). (A) Thr^{172}-phosphorylation of AMPK and GLUT4 protein levels in heart of WT and MHC-D2 mice at baseline and after DOX treatment. (B) GLUT1 protein levels in heart of MHC-D2 mice at baseline and after DOX treatment. (C) Total Akt protein levels in heart of WT mice at baseline and after DOX treatment. (D) Ser^{473}-phosphorylation of AKT in heart of WT mice. (E) Ratio of Ser^{473}-phosphorylation of AKT and total Akt protein levels in WT mice. Data are presented as means ± SE. Glyceraldehyde-3-phosphate dehydrogenase (GAPDH) served as loading controls for all data. *, $P < .05$ vs baseline.

role of BNP or other cardiomyocyte-derived factors in regulating hepatic glucose metabolism.

Heart-selective increase in T3 resulted in a two- to three-fold increase in basal myocardial glucose metabolism in MHC-D2 mice. Importantly, this increase in basal glucose uptake occurred without changes in cardiac insulin sensitivity in MHC-D2 mice. Our previous study found that chronic activation of Akt selectively in heart using MHC promoter significantly enhanced basal myocardial glucose metabolism in mice (22). Akt activation also blunted cardiomyocyte apoptosis following transient ischemia and improved cardiac function in mice (33). However, in that model, chronic Akt activation caused a negative feedback inhibition of insulin receptor substrate and phosphatidylinositol 3-kinase activity and down-regulated insulin-stimulated glucose uptake in heart (34). In MHC-D2 mice, it is likely that myocardial glucose metabolism is enhanced partly due to increased energy demand, and this does not affect insulin signaling in heart. This notion is further supported by a significant elevation in myocardial lipid levels, suggesting increased myocardial energetics, in MHC-D2 mice (14). These data are also consistent with increases in myocardial D2 activity and T3 levels in MHC-D2 mice (14). Thus, increased myocardial glucose metabolism in MHC-D2 mice may be attributed to combined effects of thyroid hormone action and enhanced cardiac work in these mice. Although these data implicate beneficial effects of local T3 activation in heart, a recent study from Wang et al found that *Dio2* up-regulation exacerbated dilated cardiomyopathy model in mice (35). Clearly, additional studies are needed to understand the molecular effects of cardiac-specific metabolic changes in normal and pathological heart conditions.

DOX, also known as Adriamycin, is an anthracycline antibiotic that is commonly used in the treatment of a wide range of cancers including hematological and breast carcinoma (36). The undesirable cardiotoxicity effects of DOX have limited its potential therapeutic use in treating cancer. Our findings indicate that DOX-mediated cardiotoxicity involves a significant increase in myocardial glucose metabolism. In that regard, it is possible that DOX-induced cardiac dysfunction is activating fetal programming in heart, which results in a significant increase in cardiac glucose utilization. In MHC-D2 mice, the constitutive increase in basal cardiac glucose utilization was more pronounced following DOX treatment, and this was associated with improved cardiac function and survival rate in these mice. These results are consistent with other findings that DOX-mediated cardiac injury is related to impaired myocardial energetics and ATP loss and cardiomyocyte apoptosis (20, 37).

In heart, AMPK serves as a key energy sensor and is activated during myocardial ischemia in response to an increased AMP/ATP ratio (38). AMPK potently regulates glucose metabolism by increasing myocardial expression of glucose transporters and stimulates translocation of glucose transporters from an intracellular pool to the plasma membrane (39). Our data indicate that DOX-mediated increase in myocardial glucose metabolism is in part due to enhanced AMPK activity, particularly in MHC-D2 heart where DOX treatment resulted in more than a six-fold increase in AMPK phosphorylation. Increased AMPK activity led to a two-fold increase in myocardial expression of GLUT1 in DOX-treated MHC-D2 mice. Additionally, myocardial expression of total Akt and Akt phosphorylation were significantly elevated in WT heart following DOX treatment, and this is consistent with our previous finding of increased myocardial glucose metabolism in mice with constitutively active Akt (22). Taken together, these results demonstrate potent effects of DOX-induced cardiac dysfunction and D2 on metabolic signaling pathways and glucose metabolism in heart.

Overall, cardiac-specific increases in T3 with human D2 expression caused an up-regulation of myocardial glucose utilization without changes in cardiac insulin sensitivity. Also, MHC-D2 mice showed a partial protection against DOX-mediated cardiac dysfunction and death. Because impaired glucose metabolism is a characteristic feature of cardiac hypertrophy and heart failure (40), our findings identify D2 as a potential therapeutic target in pathological heart conditions.

Acknowledgments

Address all correspondence and requests for reprints to: Dr Jason K. Kim, University of Massachusetts Medical School, Program in Molecular Medicine, 368 Plantation Street, Sherman Center, AS9.1041, Worcester, Massachusetts 01605. E-mail: jason.kim@umassmed.edu.

This study was supported by grants from the United States Public Health Service (R01-DK080756, R01-DK079999, R24-DK090963, and U24-DK093000 to J.K.K., and R01-DK44128 to P.R.L.), American Heart Association Grant-in-Aid (0855492D to J.K.K.), and American Diabetes Association Research Award (7-07-RA-80 to J.K.K.).

Disclosure Summary: The authors have nothing to declare.

References

1. **Grundy SM, Benjamin IJ, Burke GL, et al.** Diabetes and cardiovascular disease: a statement for healthcare professionals from the American Heart Association. *Circulation*. 1999;100:1134–1146.

2. **Gray S, Kim JK.** New insights into insulin resistance in the diabetic heart. *Trends Endocrinol Metab*. 2011;22:394–403.
3. **Stanley WC, Lopaschuk GD, McCormack JG.** Regulation of energy substrate metabolism in the diabetic heart. *Cardiovascular Res*. 1997;34:25–33.
4. **Ardehali H, Sabbah HN, Burke MA, et al.** Targeting myocardial substrate metabolism in heart failure: potential for new therapies. *Eur J Heart Fail*. 2012;14:120–129.
5. **Yen PM.** Physiological and molecular basis of thyroid hormone action. *Physiol Rev*. 2001;81:1097–1142.
6. **Weinstein SP, O'Boyle E, Haber RS.** Thyroid hormone increases basal and insulin-stimulated glucose transport in skeletal muscle. The role of GLUT4 glucose transporter expression. *Diabetes*. 1994; 94:1185–1189.
7. **Havekes B, Sauerwein HP.** Adipocyte-myocyte crosstalk in skeletal muscle insulin resistance; is there a role for thyroid hormone. *Curr Opin Clin Nut Metab Care*. 2010;13:641–646.
8. **Soriguer F, Valdes S, Morcillo S, et al.** Thyroid hormone levels predict the change in body weight: a prospective study. *Eur J Clin Invest*. 2011;41:1202–1209.
9. **Holness MJ, Greenwood GK, Smith ND, Sugden MC.** PPARα activation and increased dietary lipid oppose thyroid hormone signaling and rescue impaired glucose-stimulated insulin secretion in hyperthyroidism. *Am J Physiol Endocrinol Metab*. 2008;295: E1380–E1389.
10. **Mentuccia D, Proietti-Pannunzi L, Tanner K, et al.** Association between a novel variant of the human type 2 deiodinase gene Thr92Ala and insulin resistance: evidence of interaction with the Trp64Arg variant of the β-3-adrenergic receptor. *Diabetes*. 2002;51:880–883.
11. **de Jesus LA, Carvalho SD, Ribeiro MO, et al.** The type 2 iodothyronine deiodinase is essential for adaptive thermogenesis in brown adipose tissue. *J Clin Invest*. 2001;108:1379–1385.
12. **Marsili A, Aguayo-Mazzucato A, Chen T, et al.** Mice with targeted deletion of the type 2 deiodinase are insulin resistant and susceptible to diet induced obesity. *PLoS ONE*. 2011;6(6):e20832.
13. **Biondi B, Palmieri EA, Lombardi G, Fazio S.** Effects of thyroid hormone on cardiac function: the relative importance of heart rate, loading conditions, and myocardial contractility in the regulation of cardiac performance in human hyperthyroidism. *J Clin Endocrinol Metab*. 2002;87:968–974.
14. **Pachucki J, Hopkins J, Peeters R, et al.** Type 2 iodothyronine deiodinase transgene expression in the mouse heart causes cardiac-specific thyrotoxicosis. *Endocrinology*. 2001;142:13–20.
15. **Carvalho-Bianco SD, Kim BW, Zhang JX, et al.** Chronic cardiac-specific thyrotoxicosis increases myocardial β-adrenergic responsiveness. *Mol Endocrinol*. 2004;18:1840–1849.
16. **Lipshultz SE, Colan SD, Gelber RD, Perez-Atayde AR, Sallan SE, Sanders SP.** Late cardiac effects of doxorubicin therapy for acute lymphoblastic leukemia in childhood. *N Engl J Med*. 1991;324: 808–815.
17. **Singal PK, Li T, Kumar D, Danelisen I, Iliskovic N.** Adriamycin-induced heart failure: mechanism and modulation. *Mol Cell Biochem*. 2000;207:77–86.
18. **Volkova M, Palmeri M, Russell KS, Russell RR.** Activation of the aryl hydrocarbon receptor by doxorubicin mediates cytoprotective effects in the heart. *Cardiovascular Res*. 2011;90:305–314.
19. **Das A, Durrant D, Mitchell C, et al.** Sildenafil increases chemotherapeutic efficacy of doxorubicin in prostate cancer and ameliorates cardiac dysfunction. *PNAS*. 2010;107:18202–18207.
20. **Soni H, Pandya G, Patel P, Acharya A, Jain M, Mehta AA.** Beneficial effects of carbon monoxide-releasing molecule-2 (CORM-2) on acute doxorubicin cardiotoxicity in mice: role of oxidative stress and apoptosis. *Toxicol Appl Pharmacol*. 2011;253:70–80.
21. **Kim HJ, Higashimori T, Park SY, et al.** Differential effects of interleukin-6 and -10 on skeletal muscle and liver insulin action in vivo. *Diabetes*. 2004;53:1060–1067.
22. **Matsui T, Nagoshi T, Hong EG, et al.** Effects of chronic Akt activation on glucose uptake in the heart. *Am J Physiol Endocrinol Metab*. 2006;290:E789–E797.
23. **Park SY, Cho YR, Kim HJ, et al.** Unraveling the temporal pattern of diet-induced insulin resistance in individual organs and cardiac dysfunction in C57BL/6 mice. *Diabetes*. 2005;54:3530–3540.
24. **Berul CI.** Electrophysiological phenotyping in genetically engineered mice. *Physiol Genomics*. 2003;13:207–216.
25. **Wakimoto H, Maguire CT, Kovoor P, et al.** Induction of atrial tachycardia and fibrillation in the mouse heart. *Cardiovasc Res*. 2001;50:463–473.
26. **Young LH, Li J, Baron SJ, Russell RR.** AMP-activated protein kinase: a key stress signaling pathway in the heart. *Trends Cardiovasc Med*. 2005;15:110–118.
27. **Laville M, Riou JP, Bougneres PF, et al.** Glucose metabolism in experimental hyperthyroidism: intact in vivo sensitivity to insulin with abnormal binding and increased glucose turnover. *J Clin Endocrinol Metab*. 1984;58:960–965.
28. **Brunetto EL, Teixeira Sda S, Giannocco G, Machado UF, Nunes MT.** T3 rapidly increases SLC2A4 gene expression and GLUT4 trafficking to the plasma membrane in skeletal muscle of rat and improves glucose homeostasis. *Thyroid*. 2012;22:70–79.
29. **Castillo M, Hall JA, Correa-Medina M, et al.** Disruption of thyroid hormone activation in type 2 deiodinase knockout mice causes obesity with glucose intolerance and liver steatosis only at thermoneutrality. *Diabetes*. 2011;60:1082–1089.
30. **Klein LJ, Visser FC.** The effect of insulin on the heart: Part 1: Effects on metabolism and function. *Neth Heart J*. 2010;18:197–201.
31. **Bordicchia M, Liu D, Amri EZ, et al.** Cardiac natriuretic peptides act via p38 MAPK to induce the brown fat thermogenic program in mouse and human adipocytes. *J Clin Invest*. 2012;122:1022–1036.
32. **Welsh P, McMurray JJ.** B-type natriuretic peptide and glycaemia: an emerging cardiometabolic pathway? *Diabetologia*. 2012;55:1240–1243.
33. **Matsui T, Tao J, Monte FD, et al.** Akt activation preserves cardiac function and prevents injury after transient cardiac ischemia in vivo. *Circulation*. 2001;104:330–335.
34. **Nagoshi T, Matsui T, Aoyama T, et al.** PI3K rescues the detrimental effects of chronic Akt activation in the heart during ischemia/reperfusion injury. *J Clin Invest*. 2005;115:2128–2138.
35. **Wang Y-Y, Morimoto S, Du C-K, et al.** Up-regulation of type 2 iodothyronine deiodinase in dilated cardiomyopathy. *Cardiovascular Res*. 2010;87:636–646.
36. **Hortobágyi GN.** Anthracyclines in the treatment of cancer. An overview. *Drugs*. 1997;54:1–7.
37. **Pointon AV, Walker TM, Phillips KM, et al.** Doxorubicin in vivo rapidly alters expression and translation of myocardial electron transport chain genes, leads to ATP loss and caspase 3 activation. *PLoS One*. 2010;5(9):e12733.
38. **Russell RR III, Li J, Coven DL, et al.** AMP-activated protein kinase mediates ischemic glucose uptake and prevents postischemic cardiac dysfunction, apoptosis, and injury. *J Clin Invest*. 2004;114:495–503.
39. **Russell RR 3rd, Bergeron R, Shulman GI, Young LH.** Translocation of myocardial GLUT-4 and increased glucose uptake through activation of AMPK by AICAR. *Am J Physiol*. 1999;277:H643–H649.
40. **Mori J, Basu R, McLean BA, et al.** Agonist-induced hypertrophy and diastolic dysfunction are associated with selective reduction in glucose oxidation: a metabolic contribution to heart failure with normal ejection fraction. *Circ Heart Fail*. 2012;5:493–503.